Complex-energy analysis of intrinsic lifetimes of resonances in biased multiple quantum wells

Mathias Wagner* and Hiroshi Mizuta
Central Research Laboratory, Hitachi, Ltd., Kokubunji-Shi, Tokyo 185, Japan
(Received 16 June 1993)

The electric-field-dependent intrinsic lifetimes of resonances in biased multiple quantum wells are studied by using a complex-energy analysis based on an Airy-function transfer-matrix description of tunneling. Special attention is paid to the case when at some particular electric field two resonances belonging to different quantum wells resonantly align in energy. Two different characteristic behaviors were found in such electric-field sweeps: Long-lived resonances typically exhibit an anticrossing of their quasieigenenergies and a corresponding crossing of their lifetimes, usually associated with large changes in these lifetimes over many orders of magnitude, while short-lived resonances feature a crossing of their quasieigenenergies and an anticrossing of their lifetimes with less variation in these lifetimes. The parameters relevant for these two different regimes are discussed, and a simple model is derived to describe the crossover between these regimes.

I. INTRODUCTION

Among the physical properties explored in nanoscale heterostructures, such as resonant tunneling diodes (RTD) or multiple quantum wells (MQW), the intrinsic lifetime of electronic resonances is of fundamental interest both to the study of quantum mechanics as well as to the design of applications where a rapid charging or discharging of these resonances is of high importance, as is the case in high-frequency devices. Resonances occur in these structures since the typical vertical length scale is comparable to the electron wavelength. The present paper deals with a simple way of calculating the *intrinsic* lifetime of these resonances due to tunneling in the absence of any many-particle interaction.

Experimentally, lifetimes of resonances can be studied by measuring the sweep-out times of photogenerated carriers in RTD's or MQW's, for instance, with the help of time-resolved photoluminescence spectroscopy,[1–3] or time-resolved electroabsorption measurements.[4,5] Though it is fairly difficult to establish a rigorous connection between what is measured and the intrinsic lifetime,[6] a thorough understanding of the intrinsic lifetime is certainly a big step forward. So far, a number of methods have been employed to calculate the intrinsic lifetime of resonances in these structures.[7] Apart from various semiclassical[8–13] or wave-packet[14] approaches, probably the easiest and most often used method is based on a line-shape analysis of the transmission probability of the so-called scattering states.[2,4,15–17] These states are defined as having an incident plane wave of given wave vector k; upon reaching the structure, part of the wave is reflected while the rest can pass as the transmitted wave. By definition, there is no incident wave on the transmitted side. As in nuclear physics, by sending such a continuous wave onto the structure one can probe internal resonances of the system when varying the energy of the incident beam. When the energy of the incident wave hits a resonance, the transmission probability T is greatly enhanced, approaching unity under certain conditions. The linewidth Γ of such a peak in T is associated with the lifetime of the resonance via $\tau = \hbar/\Gamma$. This method works fairly well in simple cases, but it has a number of serious drawbacks when applying it to more complicated structures. First, the stated relation between the linewidth Γ and the lifetime τ of the resonance is exact only as long as the line shape of $T(E)$ is strictly Lorentzian. Second, this analysis can only be used for resonances with energies above the conduction-band edges in *both* contacts, as otherwise the transmission probability will vanish identically. And finally, related to the first point, if some resonances lie very close to each other in energy, it becomes impossible to extract their exact position on the basis of $T(E)$ alone; ambiguities in the line-shape fitting will always remain. In particular this last point renders many interesting effects inaccessible to the line-shape-analysis method. On the other hand, there exist a couple of approaches based on more sophisticated methods, such as, for instance, the tunneling-Hamiltonian formalism,[6] but even when assuming a constant mass throughout the structure, this formalism is still too involved to be easily used for the analysis of complex structures.

A very elegant and simple-to-use extension of the line-shape analysis of $T(E)$ is the complex-energy method, which has already been successfully applied to single quantum wells.[6,18,19] Other applications include the study of resonances in oscillating barriers,[20] T-shaped quantum wires,[21] and there has also been an attempt to utilize this method to describe inelastic scattering in double-barrier structures.[22] Basically, in this approach one considers appropriately defined scattering states having *complex* energies. The transmission amplitude $t(E)$ of these states has *poles* in the complex-energy plane.

0163-1829/93/48(19)/14393(14)/$06.00

For each pole, the real part of the pole's position defines the quasieigenenergy of a resonance, while the imaginary part is inversely proportional to its intrinsic lifetime.

In this paper we present a complete analysis of the intrinsic lifetimes of resonances in MQW's and RTD's as a function of an applied electric field. In contrast to previous approaches, we use the exact Airy-function solutions in the case of finite electric fields. Moreover, all possible boundary conditions for resonances are discussed. Particular attention is paid to the field dependence of intrinsic lifetimes when two different resonances come close to each other. If both resonances are strongly bound, an *anticrossing* with large "dips" in the lifetimes occurs as the electric field is swept. In contrast, for weakly bound levels we find that they usually undergo a *crossing* instead of an anticrossing, and that the "dips" in their lifetimes are generally much smaller or even completely absent. These findings have, for instance, implications for the analysis of carrier sweep-out rates, as they indicate intrinsic limits on the detectability of resonances in sweep-out rates even if otherwise perfect conditions are assumed. And finally, we will briefly discuss what happens when — for example, under the application of an electric field — the real part of the quasieigenenergy of a resonance crosses the conduction-band edge in the emitter or the collector contact, in which case the boundary condition for this resonance changes.

II. COMPLEX-ENERGY TRANSFER-MATRIX FORMULATION

The complex-energy method is basically the linear-system theory of classical mechanics applied to quantum-mechanical scattering states. Given a linear system

$$\psi^{\text{out}}(E) = t(E)\psi^{\text{in}}(E) \tag{2.1}$$

defining a relation between the input amplitude ψ^{in} and the output amplitude ψ^{out} as a function of energy (classically, the frequency), the eigenenergies of this system can be obtained by searching for the poles of $t(E)$ in the complex-energy plane. Equivalently, and numerically more conveniently, one can look for the roots of $1/t(E)$. At such a pole, respectively, root, the system has nontrivial solutions with *finite* output amplitude even for *vanishing* input amplitude, which can be interpreted as describing *decaying* quantum levels having only *outgoing* flux (see Fig. 1). The real part of the pole position then gives the quasieigenenergy of the decaying quantum level, while the imaginary part is related to its lifetime (classically, the damping factor γ of the resonance).

As such, the complex-energy method is simply a convenient mathematical tool which is not limited to poles having small (on whatever scale) imaginary energies, yet one has to check carefully whether the resonances found this way have anything to do with the physical resonances in the system. In the following we summarize the basic physical properties of a scattering state having a complex energy: First, by definition, it solves the Schrödinger equation with a complex eigenenergy,

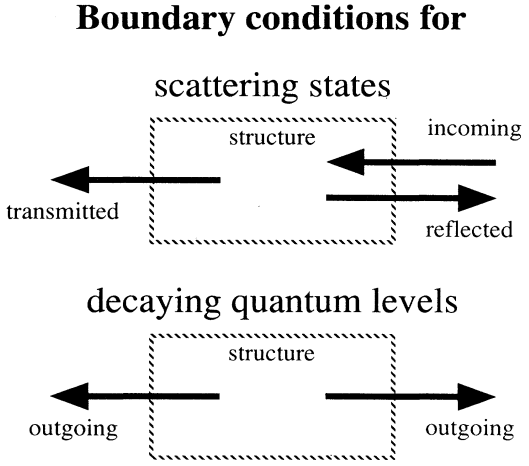

FIG. 1. Schematic boundary conditions for scattering states and decaying quantum levels (resonances). The former are defined as having an incoming, a reflected, and a transmitted wave, while the latter have only outgoing fluxes to both sides. At a pole in the complex-energy plane, the input amplitude of a scattering state goes to zero relative to the reflected and transmitted amplitudes, and hence for this particular complex energy the scattering state also satisfies the boundary condition for a decaying quantum level.

$$i\hbar\frac{\partial}{\partial t}\psi(z,t) = H(z)\psi(z,t) = \left(E - i\frac{\Gamma}{2}\right)\psi(z,t)\ . \tag{2.2}$$

At any point in space it decays exponentially as

$$\hbar\frac{\partial}{\partial t}\left|\psi(z,t)\right|^2 = -\Gamma\left|\psi(z,t)\right|^2, \tag{2.3}$$

which defines its intrinsic lifetime to be $\tau = \hbar/\Gamma$. It should be noted that for complex eigenenergies this wave function usually *cannot be normalized* as it diverges at $z \to \pm\infty$.[23] This makes an interpretation of Eq. (2.3) as describing the decay of a *localized* level not straightforward. However, in the case of a "good" resonance, the wave function has a very large amplitude somewhere within the structure as compared to its amplitude at the contacts, and it is in this sense that we can speak of localized wave functions. Introducing such a cutoff at the contacts can be justified by the randomization properties of the contacts. Another problem when comparing with experiments is that even though the resonances are localized in the system, on a quantum-well length scale they may be rather delocalized, occupying, for instance, two or more quantum wells. We do not consider how photogenerated carriers relax into such a delocalized level, but rather assume this process to have already happened. In general, we believe that with increasing imaginary eigenenergy it becomes more and more difficult to actually prepare a carrier in this level or only close to it. But even if this preparation cannot be done completely, a knowledge of the complex-energy resonances is useful as they completely characterize the analytic properties of the transmission amplitude $t(E)$, and thus the system.

It is easily seen that in the limit of infinite lifetimes the standard line-shape analysis of the transmission proba-

bility $T = tt^*$ gives exactly the same quasieigenenergy and intrinsic lifetime as the complex-energy method. In the neighborhood of a single pole at complex energy E_0 (which is always a first-order pole), $t(E)$ can be approximately written as

$$t(E) = \frac{A}{E - E_0} , \tag{2.4}$$

with some constant A. On the real axis this has the form

$$t(E) = \frac{A}{[E - \mathrm{Re}(E_0)] - i\,\mathrm{Im}(E_0)} , \tag{2.5}$$

which yields a Lorentzian line shape for T with the resonance position at $\mathrm{Re}(E_0)$ and a half linewidth of $\mathrm{Im}(E_0)$. Equation (2.5) is exact in the limit $\mathrm{Im}(E_0) \to 0$, i.e., for infinite lifetimes.

From this point on we will be more specific about the functional form of the transmission amplitude $t(E)$. We assume an effectively one-dimensional two-terminal device with an almost arbitrary internal electrostatic potential distribution, the only restriction being that the potential in the contacts is kept flat. This restriction is necessary if we want to define boundary conditions for the scattering states in terms of eigenstates of the current operator, i.e., in terms of plane waves.

In this case, four different kinds of resonances with three different boundary conditions can be distinguished. First, there is the truly bound quantum level with an eigenenergy below the conduction-band edges in either contact, resulting in an infinite lifetime. Second, there are semi-bound levels with quasieigenenergies between the collector and the emitter conduction-band edge. The quantum levels belonging to the third class, which we will call quasibound levels, have quasieigenenergies above the conduction-band edges in both contacts, but are still confined by some potential barriers in the system. Finally, virtually bound levels are unconfined towards at least one contact and have even higher quasieigenenergies than quasibound levels. A distinction between the last two types is somewhat arbitrary as they satisfy the same boundary conditions, but nevertheless it is a useful approach in view of their vastly different lifetimes. All but the quantum levels belonging to the first class have finite lifetimes.

In order to specify proper boundary conditions, the standard procedure is to decompose a scattering state of energy E in the contacts as

$$\psi_{l,r}(z) = A_{l,r} \exp(k_{l,r} z) + B_{l,r} \exp(-k_{l,r} z) , \tag{2.6}$$

where $k_{l,r} = \hbar^{-1}\sqrt{2m_{l,r}(V_{l,r} - E)}$ is the wave vector in the left (right) contact. This decomposition holds not only for plane waves [i.e., for $\mathrm{Re}(V_{l,r} - E) < 0$], but also for the case of evanescent modes with $\mathrm{Re}(V_{l,r} - E) > 0$, and one can thus treat all possible cases on the same footing.

A standard transfer matrix relates the scattering-state coefficients A and B in one contact with those of the other contact,

$$\begin{pmatrix} A_r \\ B_r \end{pmatrix} = T^{l\to r} \begin{pmatrix} A_l \\ B_l \end{pmatrix} . \tag{2.7}$$

In the Appendix details are given for how to calculate the 2×2 transfer matrix $T^{l\to r}$ for finite, piecewise constant electric fields. The standard scattering states can be obtained from this general formula by choosing the coefficients A and B in either the left- or the right-hand contact such that at this side only an *outgoing* plane-wave component exists (compare Fig. 1). The other side will then consist of an incoming plane wave and a reflected part (again, in the case of evanescent modes these boundary conditions have to be suitably modified in an obvious fashion). To describe a *decaying* level, one has to impose different boundary conditions. By definition, a decaying level has only outgoing but no incoming flux (see Fig. 1). Usually, this requirement on the coefficients cannot be met by using real energies of the scattering states alone: one has to use complex energies. Finding scattering states having complex energies such that the boundary conditions for decaying levels are met is what the complex-energy method is concerned with. Throughout the paper we will assume the incident wave to be on the right-hand side of the structure. Some of the following results are well known from standard textbooks on quantum mechanics but are repeated here for the sake of completeness.

For *truly bound levels* the boundary condition is that the wave function must not diverge for $z \to \pm\infty$, and thus we have to require $B_l = 0$ and $A_r = 0$. With our choice of scattering states, the condition $B_l = 0$ is already satisfied by definition. For the remaining condition we think of A_r as a vanishing input amplitude, and set up an equation in the spirit of Eq. (2.1) as $A_r = T_{11}^{l\to r} A_l$. [To be precise, this is the inverse of Eq. (2.1).] Then the condition $A_r = 0$ is satisfied at roots of $T_{11}^{l\to r}(E)$, i.e., at complex-energy poles of $1/T_{11}^{l\to r}$. As expected for truly bound levels, these roots always lie on the real-energy axis, yielding infinite lifetimes for these levels. For the discussion of *semi-bound* levels we take the potential in the left-hand contact to be higher than that in the right-hand contact. Then a decaying level has to satisfy the boundary condition that its wave function must not diverge in the left contact, and that on the right-hand side it may contain outgoing plane waves only. This requires $B_l = 0$ and $B_r = 0$, where again the first condition is automatically fulfilled because of our definition of the scattering states. To meet the second condition we now utilize $B_r = T_{21}^{l\to r} A_l$, and thus find that for this type of boundary condition the roots of $T_{21}^{l\to r}(E)$ are relevant. Similarly, *quasibound* and *virtually bound* quantum levels, having only outgoing flux, have to satisfy $A_l = 0$ and $B_r = 0$, and with the relation $B_r = T_{22}^{l\to r} B_l$ we see that in order to match both conditions we have to search for the roots of $T_{22}^{l\to r}(E)$.

These boundary conditions ensure that all types of resonances have only *outgoing flux* in the contact regions (or none if their energy is below the respective conduction-band edge), and thus describe *decaying* quantum levels. With $2\,\mathrm{Im}(k) \approx \Gamma m/\mathrm{Re}(k) = \Gamma/v_z$ we then find that the *total* derivative of the probability function vanishes

to first order in the contact layers,

$$\frac{d}{dt}|\psi(z)|^2 = \frac{\partial}{\partial t}|\psi(z)|^2 + v_z\frac{\partial}{\partial z}|\psi(z)|^2$$
$$= -\Gamma|\psi(z)|^2 + v_z 2\,\mathrm{Im}(k)\,|\psi(z)|^2$$
$$= 0\,. \qquad (2.8)$$

The physical interpretation is simple: in the time frame of the moving particle it cannot decay, and the probability is therefore conserved.

As a final remark we note that apart from poles below the real-energy axis, there are mirrored poles above this axis too, which correspond to growing resonances having only *incoming* fluxes.

III. A DOUBLE QUANTUM WELL

Under an electric field, the relative positions of quantum levels in a double quantum well (or more generally a MQW) shift strongly when the levels belong to different wells. Most of this shift is due to the bottom of the respective quantum well being raised or lowered by the field, while a small fraction stems from the Stark effect. In this way, for some electric field the first level of a well can be made to align with the second level of the neighboring well, a method which is, for example, used in sequential tunneling devices. In this section we will study the behavior of the intrinsic lifetime of quantum levels when they experience a resonance caused by such an alignment. The main features can already be investigated in a double quantum-well system, but we have tested this method for as many as six coupled quantum wells.

A. Truly bound levels

The eigenenergies of truly bound levels can never cross each other, even if they belong to different quantum wells off resonance. The reason is simply that the number of nodes of the wave function, and hence the energetic ordering of these wave functions, is conserved and cannot be changed by the electric field. As an example consider the buried double-well structure of Fig. 2(a) where each quantum well can accommodate two truly bound quantum levels at zero bias. Throughout the paper, our convention is that the quantum levels are labeled as $E_1, E_2, E_3, \ldots$ in order of increasing energy at *zero bias*. When for increasing electric field F the eigenenergy of the first level in the left-hand well, marked E_2, is sufficiently close to the energy of the E_3 level in the right-hand well, both levels will start to delocalize within the two quantum wells. At resonance, the levels are maximally delocalized,[24] and further increasing the electric field leads to both levels localizing again. Eventually, all the probability of the E_2 level will have moved to the right well, while the E_3 level can now be found in the left well. This transition process is illustrated in Figs. 2(b)–2(d), showing the probability function $|\psi(z)|^2$ of these levels just before (b), at (c), and after (d) resonant alignment (where the electric field at resonance, F_R, is defined as the field at which the separation between the eigenen-

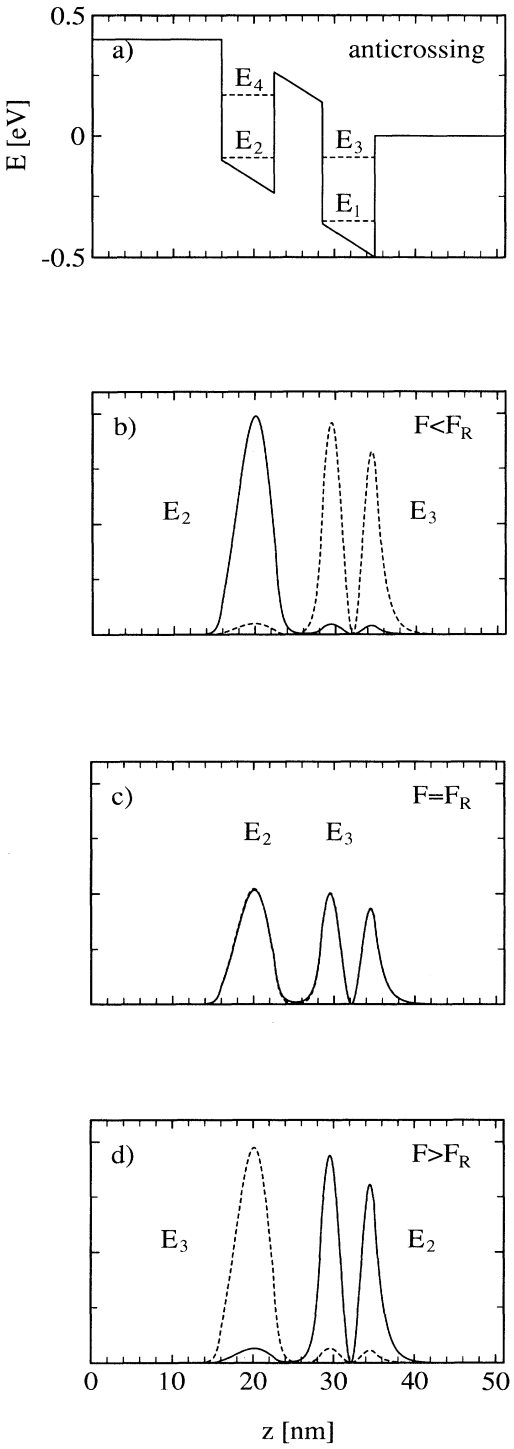

FIG. 2. Four quantum levels in a buried double quantum-well structure (L_W =65 Å, L_B =60 Å, m_W = $0.0436m_0$, m_B = $0.0836m_0$, V_B = 500 meV). Under an applied electric field of F_R = 210.5 kV/cm, the levels E_2 of the left-hand well and E_3 of the right-hand well (both of which are truly bound) come to resonance (a). (b)–(d) show the normalized probability function $|\psi(z)|^2$ just before (b), at (c), and after (d) resonance. The swapping of positions is characteristic for an *anticrossing* behavior in the electric-field sweep as seen in Fig. 3.

ergies of levels E_2 and E_3 is minimal). Such a behavior corresponds to an *anticrossing* in the electric-field sweep as can be seen in Fig. 3 at 210.5 kV/cm. In this figure, as well as in all following, the energies are always measured with respect to the collector conduction-band edge which is taken to be zero.

B. Strongly bound levels

As can be expected, *strongly* bound quantum levels with finite but very long lifetimes behave similarly to truly bound levels. Figure 4(a) shows a characteristic double-well structure of 65-Å-wide quantum wells bound by 60-Å tunneling barriers under an applied electric field of F_R =207 kV/cm, where resonance between the E_2 and E_3 levels occurs. Note that the electric field extends only over a finite range, the potentials in the left and right contacts are kept flat. At the bias shown all four quantum levels belong to the category of semi-bound levels as their quasieigenenergies lie between the potentials of the left and the right contacts. These quasieigenenergies have been determined from the real part of the pole position in the complex energy as described in the preceding section. Again, Figs. 4(b)–4(d) display the squared amplitude $|\psi(z)|^2$ before (b), at (c), and after resonance (d).[25] As in the case of truly bound levels, the levels E_2 and E_3 swap positions at resonance which is typical for an *anticrossing* of the quasieigenenergies in an electric-field sweep, as is exemplified in Fig. 5(a).

Having an energy higher than the conduction-band edge in the collector contact, an electron placed in one of these quantum levels can tunnel through the barriers towards the collector contact. The lifetime associated with this process, the intrinsic lifetime, is a function of the electric field. In general it decreases with increasing electric field since the effective barrier heights on the collector side become smaller for larger fields. In fact, far away from other resonances, the lifetime depends exponentially on the electric field, as can, for instance, be seen in Fig.

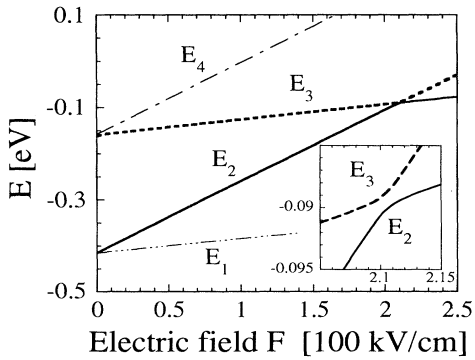

FIG. 3. Shown are the energy shifts of the four quantum levels E_1–E_4 of Fig. 2 as a function of the applied electric field F (the potentials in both contacts are flat, with the collector side taken to be the reference point). Levels belonging to the same well (i.e., E_1 and E_3, and E_2 and E_4) basically have the same slope since the Stark effect is very small on this scale. At F_R = 210.5 kV/cm the levels E_2 and E_3 undergo an *anticrossing*, which is shown in more detail in the inset.

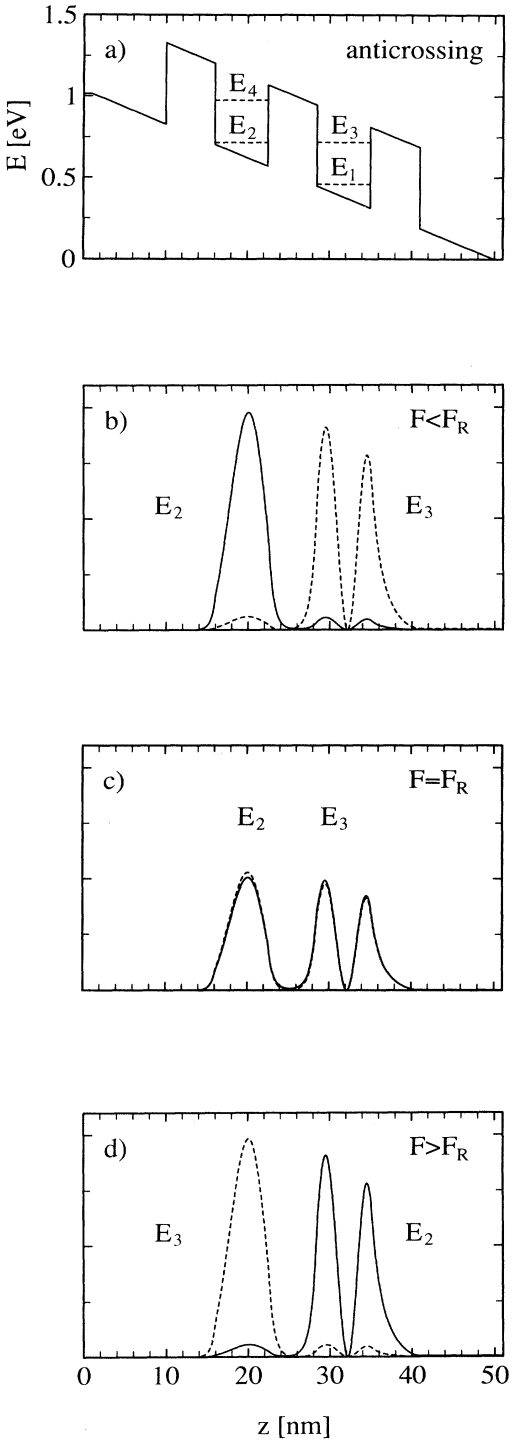

FIG. 4. Four semi-bound quantum levels in a double quantum-well structure (L_W =65 Å, L_B =60 Å, m_W = $0.0436m_0$, m_B = $0.0836m_0$, V_B = 500 meV, separated from the contacts by buffer layers of 90 Å width each). Under an applied electric field of F_R = 207 kV/cm, the levels E_2 of the left-hand well and E_3 of the right-hand well come to resonance (a). (b)–(d) show the squared amplitude $|\psi(z)|^2$ just before (b), at (c), and after (d) resonance. The swapping of positions is characteristic for an *anticrossing* behavior in the electric-field sweep as seen in Fig. 5(a).

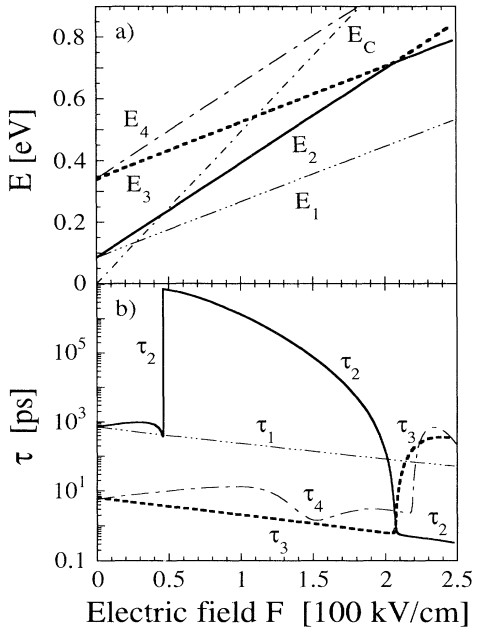

FIG. 5. (a) shows the energy shifts of the four quantum levels $E_1 - E_4$ of Fig. 4 as a function of the applied electric field F. The potential on the collector side is taken to be the reference point. The dash-dotted line labeled E_c refers to the energy of the conduction-band edge in the emitter contact. At $F_R = 207$ kV/cm the levels E_2 and E_3 undergo an *anticrossing*, which is reflected in (b), showing the intrinsic lifetimes τ_i, as a corresponding *crossing* of their lifetimes.

5(b) in the case of the E_1 and E_3 levels of the right-hand well. On the other hand, the drastic, steplike increase of the lifetime τ_2 of the E_2 level in the left-hand well at an electric field of about 46 kV/cm is due to this level dropping at this field strength below the conduction-band edge of the emitter contact, which renders the tunneling towards this side impossible. Though such a drop does in principle occur for the other levels too when they pass a conduction-band edge, it is by far strongest for the E_2 level as this level has two quite opaque barriers to the right but only one rather transparent barrier to the left. Thus electrons escape from this level primarily towards the emitter contact, and when this channel is closed the intrinsic lifetime increases by many orders of magnitude. The precise electric field at which this transition happens obviously depends on the voltage drop over the accumulation layer, which is the layer between the emitter contact and the first barrier, and hence on the length of this layer. In the present example this length was set to be 90 Å. For very thick accumulation layers, such as those used in MQW devices, the electric-field necessary to push a quantum level below the emitter conduction-band edge goes to zero, and thus for virtually all electric field strengths carriers can only tunnel to the collector contact. Another interesting behavior in the lifetimes shows up at 207 kV/cm when the E_2 and E_3 levels come to resonance. While the quasieigenenergies of these levels undergo an anticrossing, their lifetimes exhibit a crossing. The reason is simply that when the levels swap positions in coordinate space [as shown in Figs. 4(b)–4(d)], they also interchange the channels and ways to escape from these levels, i.e., their intrinsic lifetimes. This has, for example, a pronounced effect on the sweep-out rates of photogenerated carriers as measured in experiments.[4,11] If we assume that only the lowest level in each quantum well is occupied, then the lifetime of a carrier in the quasi ground state of the left quantum well will follow neither curve τ_2 nor curve τ_3 of Fig. 5(b), but approximately be given by curve τ_2 up to the point where it crosses curve τ_3, and after that by curve τ_3. The resulting line shape of the sweep-out time exhibits a strong "dip" of more than two orders of magnitude at the resonance position where the two levels align. It can therefore be concluded that the sweep-out mechanism is most effective at resonance. Finally, we note that for quasibound levels [which by definition have energies above both conduction-band edges and hence finite transmission probabilities $T(E)$] the anticrossing characteristic of the quasieigenenergies can also be seen in the transmission probability as a distinct double-peak fine structure,[26] even at resonance.

C. Weakly bound levels

The situation is quite different for *weakly* bound levels. When changing the parameters used in Fig. 4(a) only slightly to a well width of 60 Å and a barrier width of 65 Å, the resulting quasieigenenergies E_1–E_4 are slightly higher than before, making these levels less bound [see Fig. 6(a)]. In this case we find that the levels now undergo a *crossing* instead of an anticrossing in an electric-field sweep. This means that at resonance the levels no longer swap positions, but more or less remain localized in their respective wells [compare Figs. 4(b)–4(d) with Figs. 6(b)–6(d)]. Only a small delocalization is found at resonance, as seen in Fig. 6(c). The *crossing* of the quasieigenenergies as shown in Fig. 7(a) is accompanied by a corresponding *anticrossing* in the lifetimes [Fig. 7(b)]. In the case of weakly bound levels, the "dips" in the lifetime at resonance are much less pronounced than before, and may even vanish for extremely loosely bound levels.

D. Crossing versus anticrossing behavior

To understand what the relevant parameters are which determine whether two unperturbed quantum levels E_1^0 and E_2^0 will undergo a crossing or an anticrossing, we will study the standard two-level approximation to quantum resonances,[27] generalized to eigenfunctions with complex eigenenergies. (In the following, the notion "eigenenergy" refers to the standard assembly of quasieigenenergy and inverse lifetime into a complex quantity, $E - i\hbar/2\tau$.) As a basis set we take two eigenfunctions $\{|\phi_1\rangle, |\phi_2\rangle\}$ of the full Hamiltonian, one of each branch, at an electric field F_0 *slightly lower* than the field F_R at which the crossing/anticrossing occurs. The precise value of the field F_0 does not matter as long as it is sufficiently far away from the resonance field F_R so that the states $|\phi_1\rangle$ and $|\phi_2\rangle$ do not yet noticeably interact. The effective Hamiltonian $H(F)$ to be diagonalized is[28]

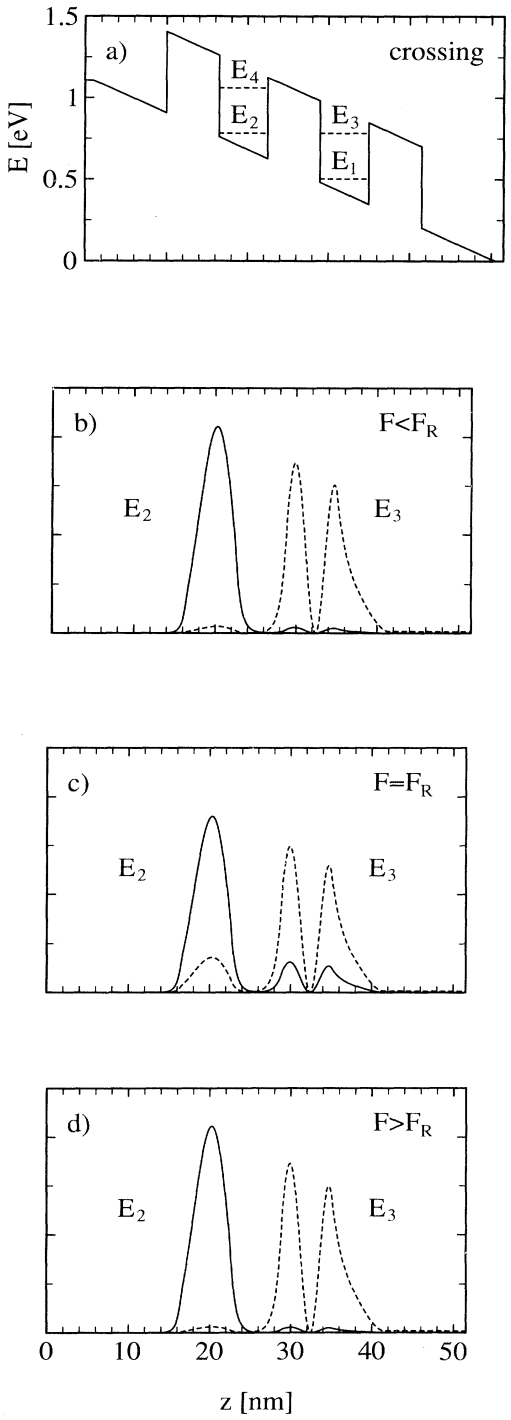

FIG. 6. Four semi-bound quantum levels in a double quantum-well structure similar to that of Fig. 4, except that now the wells are a little narrower and the barriers somewhat thicker (L_W =60 Å, L_B =65 Å). Under an applied electric field of F_R = 224 kV/cm, the levels E_2 of the left-hand well and E_3 of the right-hand well come to resonance (a). (b)–(d) show the squared amplitude $|\psi(z)|^2$ just before (b), at (c), and after (d) resonance. In contrast to the *anticrossing* case illustrated in Fig. 4, the levels now remain pretty localized even at resonance, which is characteristic for a *crossing* behavior in the electric-field sweep [as seen in Fig. 7(a)].

$$H(F) = \begin{pmatrix} \langle 1|H(F)|1\rangle & \langle 1|H(F)-H(F_0)|2\rangle \\ \langle 2|H(F)-H(F_0)|1\rangle & \langle 2|H(F)|2\rangle \end{pmatrix}. \tag{3.1}$$

The resulting (generally complex-valued) eigenenergies E^+ and E^- are

$$E^+(F) = \tfrac{1}{2}M(F) + \tfrac{1}{2}\sqrt{\Delta(F)+4W^2(F)}\,,$$
$$E^-(F) = \tfrac{1}{2}M(F) - \tfrac{1}{2}\sqrt{\Delta(F)+4W^2(F)}\,, \tag{3.2}$$

where we have introduced the "center of energy" $M(F)/2 = [\langle 1|H(F)|1\rangle + \langle 2|H(F)|2\rangle]/2$, the "relative energy" $\Delta(F) = \langle 1|H(F)|1\rangle - \langle 2|H(F)|2\rangle$, and an effective overlap integral $W^2(F) = \langle 1|H(F)-H(F_0)|2\rangle\langle 2|H(F)-H(F_0)|1\rangle$. As the electric field is increased from F_0 across F_R, the two branches E^+ and E^- shift in energy, with their real parts undergoing either a crossing or an anticrossing at resonance. For truly bound levels having only real energies the square-root expression in Eq. (3.2) is always positive, and hence $E^+(F) > E^-(F)$ holds for all electric fields in the neighborhood of the resonance. This is the *anticrossing* case: If initially, say, the unperturbed E_2^0 level is higher in energy than the E_1^0 level, then as the electric field F is increased, the E^+ branch will asymptotically evolve from the E_2^0 level towards the E_1^0 level, while the E^- branch will evolve from E_1^0 to E_2^0. In the "center of energy" frame, these two branches approximately form two repelling hyperbolas as a function of $\Delta(F)$.

In the case of quantum levels with finite lifetimes

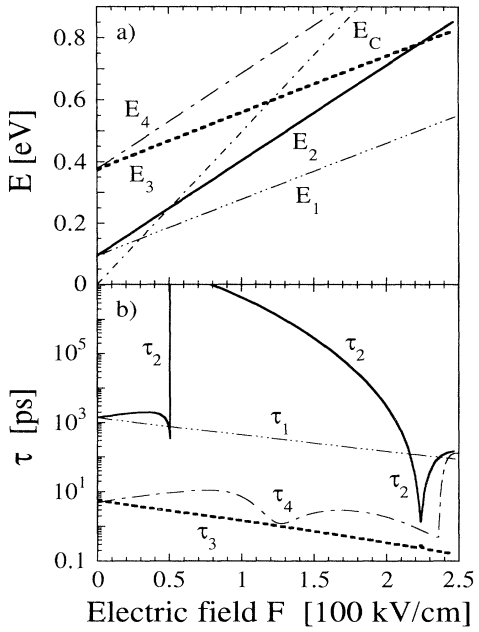

FIG. 7. Energy shifts (a) of the four quantum levels E_1 – E_4 of Fig. 6 and intrinsic lifetimes τ_i (b) as a function of the applied electric field F. Because the E_2 and E_3 levels are less bound in this case than in Figs. 4 and 5, they now undergo a *crossing* at an electric field of F_R = 224 kV/cm. This corresponds to an *anticrossing* of their lifetimes as illustrated in (b).

and consequently complex eigenenergies, the quantities $M(F)$, $\Delta(F)$, and $W^2(F)$ occurring in Eq. (3.2) become complex. If we define the cut of the square root in the complex plane to be located as usual on the negative real axis, the transition between very long-lived levels and truly bound levels will be smooth, as required. In particular, by taking the principal branch of the square root we see that for all possible complex values of the square root's argument, the real part of $\sqrt{\Delta(F)+4W^2(F)}$ will always be positive. As a consequence, we again find the relation $\mathrm{Re}[E^+(F)-E^-(F)]>0$ to hold for all electric fields in the neighborhood of the resonance, seemingly implying that quantum levels with finite lifetimes, too, will always undergo an *anticrossing* in their quasieigenenergies. However, this naive analysis does not consider the case that when increasing the electric field, the square root's argument, $\Delta(F)+4W^2(F)$, may in fact cross the cut on the negative real axis at some particular point. Continuity of the solutions then requires that from this point on the other solution of the square root having a *negative* real part has to be used. In terms of the E^+ and E^- branches this means that at this particular field strength the relation $\mathrm{Re}[E^+(F)-E^-(F)]>0$ turns into $\mathrm{Re}[E^+(F)-E^-(F)]<0$, and hence that a *crossing* of the quasieigenenergies takes place.

The crossover point between the anticrossing and the crossing regime can thus be characterized by the conditions

$$\begin{aligned}\mathrm{Re}[\Delta(F)+4W^2(F)]&=0\ ,\\ \mathrm{Im}[\Delta(F)+4W^2(F)]&=0\ .\end{aligned}\tag{3.3}$$

In the neighborhood of the resonance $\mathrm{Re}\langle 1|H(F)|1\rangle \approx \mathrm{Re}\langle 2|H(F)|2\rangle$ holds, giving

$$\mathrm{Re}[\Delta(F)]\approx -\{\mathrm{Im}[\langle 1|H(F)|1\rangle-\langle 2|H(F)|2\rangle]\}^2\ ,\tag{3.4}$$

and

$$\mathrm{Im}[\Delta(F)]\approx 0\ .\tag{3.5}$$

After having carried out a proper renormalization procedure to overcome the difficulties associated with the eigenfunctions initially not being normalizable (see Ref. 28), the imaginary part of $W^2(F)$ will be negligible, and hence the crossover point between the anticrossing and the crossing regime satisfies the relation

$$\begin{aligned}2|W(F)|&=\sqrt{-\mathrm{Re}[\Delta(F)]}\\ &\approx|\mathrm{Im}[\langle 1|H(F)|1\rangle-\langle 2|H(F)|2\rangle]|\\ &\approx|\mathrm{Im}(E_1^0-E_2^0)|\ ,\end{aligned}\tag{3.6}$$

where $\mathrm{Im}(E_1^0-E_2^0)$ is the difference in the imaginary parts of the unperturbed eigenenergies, extrapolated to the resonance region. The physical interpretation of Eq. (3.6) is simple. If the difference $|\mathrm{Im}(E_1^0-E_2^0)|$ (which is directly related to the difference in intrinsic lifetimes) is smaller than the effective overlap integral $2|W(F)|$, the levels will undergo an anticrossing, if it is larger they will cross. Thus for a given overlap integral, short-lived levels will tend to cross while long-lived levels are likely to anticross. To explicitly demonstrate that Eq. (3.2) can describe both regimes, we adopt a simple model in which the matrix elements depend linearly on the electric field as $\langle 1|H(F)|1\rangle=\alpha_1F-i(\beta_1+\gamma_1F)$, $\langle 2|H(F)|2\rangle=\alpha_2F-i(\beta_2+\gamma_2F)$ (with $\alpha_i,\beta_i,\gamma_i>0$), and $W^2(F)=$ const. For simplicity, we let the crossing take place at zero energy and zero electric field. The crossover point is then given by $2W=2W_0\equiv|\beta_1-\beta_2|$. Figure 8 shows the eigenenergies E^+, E^- and intrinsic lifetimes τ^+, τ^- as calculated from Eq. (3.2) by using some typical values for α_i, β_i, and γ_i. Figure 8(a) is representative of the anticrossing regime with $W>W_0$, while in Fig. 8(b) $W<W_0$ was assumed, which characterizes the crossing regime. Both cases clearly reproduce the typical features of the crossing (anticrossing) regime as found in the exact numerical treatment (compare, for instance, with Figs. 5 and 7).

There are two ways of turning an anticrossing into a crossing. One can either increase $|\mathrm{Im}(E_1^0-E_2^0)|$ by increasing the difference in intrinsic lifetimes, preferably by decreasing the shorter of both lifetimes or, alternatively, one can decide to reduce the effective overlap integral $W(F)$ between the states $|\phi_1\rangle$ and $|\phi_2\rangle$, for example, by increasing the barrier thickness between the two quantum wells involved.

To illustrate how the transition takes place between a crossing and an anticrossing behavior, we have looked in the *crossing regime* at the well-width dependence of the

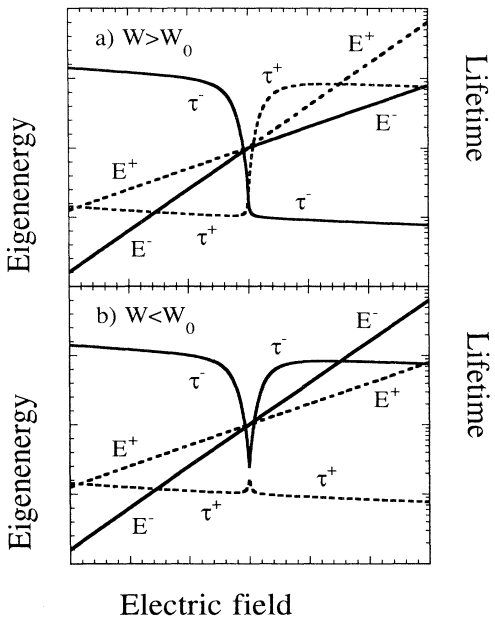

FIG. 8. Energy shifts E^+, E^- and lifetimes τ^+, τ^- as calculated from the real and imaginary parts of Eq. (3.2) when assuming that the matrix elements depend linearly on the electric field. The only difference between (a) and (b) is a variation of the overlap integral W (which is taken as a parameter). In (a) this integral is greater than the difference in the imaginary energies, W_0, leading to an anticrossing behavior of the quasieigenenergies. For (b) $W<W_0$ was assumed, resulting in a crossing.

lifetimes τ_2 and τ_3 *at resonance* in a double-well structure having otherwise the same parameters as in Fig. 6. The wider a quantum well the lower are the quasieigenenergies of the levels, and hence the stronger are the levels bound. As a result, when increasing the well widths the difference in the lifetimes τ_2 and τ_3 gets smaller. According to the discussion given above, one can therefore expect that at some well width the crossing behavior of Fig. 6 will turn into an anticrossing. Figure 9 shows such a well-width sweep for three different configurations of the barriers. For Fig. 9(a) all barrier heights were set to $V_b = 0.5$ eV as in Fig. 6. The solid curve shows the lifetime of the E_2 level at the point where this level is at resonance with the E_3 level — whose lifetime is given by the dotted curve. The crossover point between the crossing and anticrossing regime is where these two curves intersect, and is found to be at a well width of ≈ 61.35 Å. To reduce the overlap integral $W(F)$ we then increased the height of the middle barrier to $V_m = 0.53$ eV, while leaving the other barriers at 0.5 eV. The result, shown as curve (b) in Fig. 9, indeed indicates a stronger tendency of the two levels to undergo a crossing, with the effect that the crossover point between the two regimes is shifted to larger well widths (≈ 63.0 Å). It has to be said though, that this effect is not only due to the overlap integral $W(F)$ being reduced but also due to the quasieigenenergies going up for increased confinement, effectively reducing (in particular) the right-hand barrier height. On the other hand, raising only the right-hand barrier has the opposite effect. Figure 9(c) was generated using a right-hand barrier of 0.515 eV, and the crossover point is now shifted down to ≈ 59.9 Å. This can be explained in terms of a taller right-hand barrier leading to both levels, E_2 and E_3, having reduced fluxes towards the right contact, which tends to equalize their inverse lifetimes. According to the analysis given above, this makes an anticrossing of the quasieigenenergies more likely.

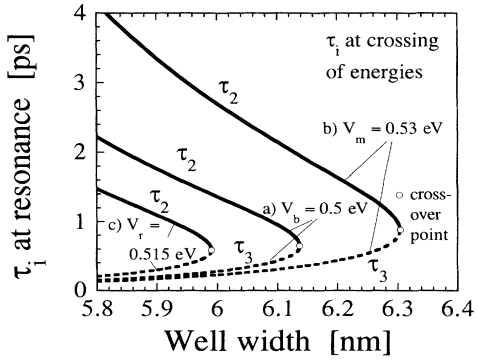

FIG. 9. Lifetimes τ_2 and τ_3 at resonance in the *crossing* regime as a function of the well width in a double-barrier structure otherwise identical to Fig. 6. As the levels become more bound for wider wells, the tendency to anticross increases, resulting in the two lifetimes approaching each other. The crossover point between the crossing and anticrossing regimes is where the τ_2 and τ_3 curves intersect (indicated as ○). For set (a), all barriers have a nominal height of 0.5 eV. In case (b) the middle barrier was raised to 0.53 eV, while in case (c) the right-hand barrier was increased to 0.515 eV. The resulting shift of the crossover point can be explained in terms of changes in the overlap integral and the difference in lifetimes (see text for details).

The results of this section resolve the problem as to whether quantum levels belonging to two different, extremely weakly coupled wells would always "see" each other at resonance if there are no phase-breaking mechanisms — regardless of the separation of the wells. They will not, as their overlap integral will be too small at large separations, and so they will simply undergo a crossing. Moreover, as the overlap integral becomes smaller and smaller, the intrinsic lifetimes will eventually display no resonance at all at the point of crossing. This is important for the analysis of MQW structures with many wells as it allows us to restrict our considerations to fairly small systems of only a few coupled quantum wells.

IV. CROSSOVER BETWEEN DIFFERENT BOUNDARY CONDITIONS

When changing parameters of the system, such as, for instance, the electric field or the width of some layers, it may happen that the boundary conditions to be satisfied by a particular quantum level may change. The question of whether or not such a transition between one boundary condition and another yields *continuous* quasieigenenergies and intrinsic lifetimes as a function of the transition parameter turns out to be very much a question of how exactly such a transition is performed. Let us first study a case where this transition is continuous.

Consider a right-hand contact which includes a thick barrier of height $E_{c'}$ and width L as illustrated in Fig. 10. A decaying quantum level of energy E (with $E_c < E < E_{c'}$) has to satisfy the boundary condition that to the right-hand side only an *outgoing* plane-wave component can exist. However, letting the barrier width L go to infinity is tantamount to changing the conduction-band edge from E_c to $E_{c'}$, i.e., to changing the boundary condition. The analysis of this transition is simple. For any finite barrier width L, the wave function in the barrier layer consists as usual of two contributions, a decaying and a divergent evanescent mode. It is easily seen that with increasing width L the *divergent* contribution in the barrier will die out, and hence that in the limit $L \to \infty$ the wave function will satisfy the proper boundary condition appropriate for $E < E_{c'}$, meaning that the transition between these two boundary conditions is smooth.[29]

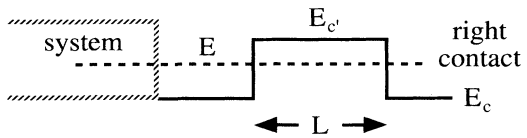

FIG. 10. Schematic right-hand contact of a "black-box" structure. The width L of the barrier layer is variable. For any finite L, the quantum level at energy $E > E_c$ has to meet the outgoing-plane-wave boundary condition, while for $L \to \infty$ the boundary condition is that the wave function decays exponentially. The transition between these two types of boundary conditions is *continuous* (see text).

On the other hand, when sweeping the electric field, the transition between boundary conditions is usually *not* smooth. The transition happens when the quasieigenenergy of a resonance (i.e., the real part of the position of the complex-energy pole) crosses the conduction-band edge in either the emitter or the collector contact, in which case the wave function in that contact changes from a plane wave to an evanescent wave or vice versa. This transition is certainly not smooth, but one has to be careful about the scale to expect for the discontinuity. For instance, such a transition may be associated with large changes in the intrinsic lifetime when that particular side on which the crossing occurred served as the main exit for decay, as we have seen, for instance, in Figs. 4–7. Nevertheless, it can be shown that this dramatic change in the lifetime is *not* discontinuous but that there is an onset of a change just before the quantum level is about to dip below the conduction-band edge. Basically, the argument relies on the outgoing flux being proportional to the k vector in that contact. When for decreasing energy this flux goes to zero, so does the probability for an electron escaping towards this contact and hence, eventually the lifetime will rapidly but smoothly change.

The "true" discontinuity when sweeping the electric field is on a much smaller scale. Our preliminary numerical results show that for a small transition regime of electric fields it may happen that the resonance at the conduction-band edge either cannot exist at all or, on the contrary, that two resonances can coexist, one with the old boundary condition and the other with the new one. Though this effect is certainly of interest in applications utilizing the stability of pinned virtually bound quantum levels in multistable coherent-electron devices,[30] it seems that the transition regime of electric fields is rather small, making an experimental observation difficult. A further analysis of this effect is under way.

V. CONCLUSIONS

A complex-energy analysis of the transition amplitude of scattering states has been utilized to calculate quasieigenenergies and intrinsic lifetimes of decaying quantum levels in semiconductor heterostructures under arbitrary bias. All possible boundary conditions for the decaying levels were studied (corresponding to their energies being below or above the conduction-band edges in the emitter and collector contacts), and the electric field was exactly taken into account by employing Airy functions in the transfer-matrix description of the scattering states. The main body of the paper had been devoted to an analysis of electric-field sweeps in double quantum-well structures, which represent the simplest case where a resonant alignment of quantum levels belonging to different wells can be achieved, but the theory presented here is also applicable to more complicated structures. Basically, two different characteristic behaviors were found. As the electric field is swept, *strongly bound* quantum levels always experience an anticrossing of their quasieigenenergies and a corresponding crossing of their lifetimes. This behavior is very well known from the treatment of *truly bound* levels in standard textbooks on quantum mechanics. On the other hand, *weakly bound* levels having a very short intrinsic lifetime generally do the opposite — they cross in quasieigenenergies and anticross with respect to their lifetimes. These two different behaviors can be explained in terms of a simple two-level model, and the relevant parameter distinguishing the two regimes is found to be the ratio of an effective overlap matrix element to the difference in the inverse intrinsic lifetimes of the two (unperturbed) levels involved. At resonant alignment, the intrinsic lifetime of the longer-lived quantum level typically changes by orders of magnitude. This is particularly the case for strongly bound quantum levels, and has been seen in a number of experiments. Finally, a better understanding of the electric-field dependence of the intrinsic lifetime is also of great value to the design of high-speed devices based on RTD's or MQW's.

ACKNOWLEDGMENTS

We are indebted to D. Moss, who brought this topic to our attention in the first place, and who continued giving us advice and very helpful comments. We thank S. Ho and K. Yamaguchi for valuable discussions and encouraging support.

APPENDIX: DEFINITION OF TRANSFER MATRICES

In this appendix the basic formulas are summarized for describing electronic resonances (i.e., truly bound, semi-bound, quasibound, and virtually bound levels) in RTD's, MQW's, and related vertical heterostructures by utilizing a transfer-matrix description of the scattering states in these structures.

1. Arbitrary electric fields

To calculate a scattering state across the whole structure, the standard approach in effective-mass approximation is to split the heterostructure into a number of layers, each layer having a constant electric field and a constant effective mass. Then the time-independent Schrödinger equation in layer I reads

$$\left\{\hbar^2 \frac{d^2}{dz^2} - 2m_{\mathrm{I}}\left(V_{\mathrm{I}} - E - F_{\mathrm{I}} z\right)\right\}\psi_{\mathrm{I}}(z) = 0 \ , \qquad \text{(A1)}$$

where m_{I}, V_{I} and F_{I} are the effective mass, the potential, and the electric field, respectively, of layer I (for convenience, the elementary charge e has been absorbed in the electric field F). For vanishing field $F_{\mathrm{I}} = 0$ the general solution is a linear combination of plane waves,

$$\psi_{\mathrm{I}}(z) = A_{\mathrm{I}} \exp(k_{\mathrm{I}} z) + B_{\mathrm{I}} \exp(-k_{\mathrm{I}} z) \ , \qquad \text{(A2)}$$

with the wave vector $\hbar k_{\mathrm{I}} = \sqrt{2m_{\mathrm{I}}(V_{\mathrm{I}} - E)}$, whereas for finite electric field the solution is a linear combination of Airy functions,

$$\psi_{\mathrm{I}}(z) = A_{\mathrm{I}}\mathrm{Ai}[Z_{\mathrm{I}}(z)] + B_{\mathrm{I}}\mathrm{Bi}[Z_{\mathrm{I}}(z)] \ , \qquad \text{(A3)}$$

with $Z_{\mathrm{I}}(z) = (2m_{\mathrm{I}}F_{\mathrm{I}})^{-2/3}(\hbar^2 k_{\mathrm{I}}^2 - 2m_{\mathrm{I}}F_{\mathrm{I}} z)$. At interfaces

between different layers I and II, the wave function has to satisfy the standard boundary conditions of continuity of the wave function and continuity of the flux,

$$\psi_{\rm I}(z_i) = \psi_{\rm II}(z_i) \ ,$$
$$\frac{1}{m_{\rm I}}\frac{\partial}{\partial z}\psi_{\rm I}(z)\Big|_{z=z_i} = \frac{1}{m_{\rm II}}\frac{\partial}{\partial z}\psi_{\rm II}(z)\Big|_{z=z_i} \ . \qquad \text{(A4)}$$

To get a transfer-matrix description of a scattering state, this is usually rewritten in terms of a matrix equation for the expansion coefficients $A_{\rm I}$, $B_{\rm I}$ of layer I and $A_{\rm II}$, $B_{\rm II}$ of layer II,

$$T^{\rm I}_{z_i}\begin{pmatrix} A_{\rm I} \\ B_{\rm I}\end{pmatrix} = T^{\rm II}_{z_i}\begin{pmatrix} A_{\rm II} \\ B_{\rm II}\end{pmatrix} \ . \qquad \text{(A5)}$$

The transfer matrix relating the coefficients of layer I across an interface located at z_i with those of layer II is then given by

$$T^{\rm I\to II}_{z_i} = \left(T^{\rm II}_{z_i}\right)^{-1} T^{\rm I}_{z_i} \ . \qquad \text{(A6)}$$

This is the standard way of defining a transfer matrix.[26] It relates the plane-wave, respectively, Airy-function expansion coefficients of the wave function in the various layers with each other (see also Fig. 11). At each interface z_i there are four different flavors of transfer matrices corresponding to the four possibilities of having zero or finite electric fields in the neighboring layers I and II: (1) the flat-flat case,

$$T^{\rm I\to II}_{z_i} = \frac{1}{2}\begin{pmatrix} \alpha\exp(k^-_{\rm I,II}z_i) & \beta\exp(-k^+_{\rm I,II}z_i) \\ \beta\exp(k^+_{\rm I,II}z_i) & \alpha\exp(-k^-_{\rm I,II}z_i)\end{pmatrix} \ , \qquad \text{(A7)}$$

with $k^\pm_{\rm I,II} = k_{\rm I} \pm k_{\rm II}$, $\hbar k_{\rm I} = \sqrt{2m_{\rm I}(V_{\rm I}-E)}$, $\alpha = 1 + \frac{k_{\rm I}m_{\rm II}}{k_{\rm II}m_{\rm I}}$ and $\beta = 1 - \frac{k_{\rm I}m_{\rm II}}{k_{\rm II}m_{\rm I}}$; (2) the field-field case (where the properties of the Wronskian of the Airy functions have been used to calculate the determinant of the inverse),

$$T^{\rm I\to II}_{z_i} = \pi\begin{pmatrix} {\rm Bi}'_{\rm II}{\rm Ai}_{\rm I} - \alpha\,{\rm Bi}_{\rm II}{\rm Ai}'_{\rm I} & {\rm Bi}'_{\rm II}{\rm Bi}_{\rm I} - \alpha\,{\rm Bi}_{\rm II}{\rm Bi}'_{\rm I} \\ \alpha\,{\rm Ai}_{\rm II}{\rm Ai}'_{\rm I} - {\rm Ai}'_{\rm II}{\rm Ai}_{\rm I} & \alpha{\rm Ai}_{\rm II}{\rm Bi}'_{\rm I} - {\rm Ai}'_{\rm II}{\rm Bi}_{\rm I}\end{pmatrix} , \qquad \text{(A8)}$$

with ${\rm Ai}_{\rm I} = {\rm Ai}(Z_{\rm I})$, $Z_{\rm I} = (2m_{\rm I}F_{\rm I})^{-2/3}(\hbar^2k_{\rm I}^2 - 2m_{\rm I}F_{\rm I}z_i)$ (similar definitions hold for the other Airy functions, and for $Z_{\rm II}$), and $\alpha = (m_{\rm I}F_{\rm I}/m_{\rm II}F_{\rm II})^{1/3}\frac{m_{\rm II}}{m_{\rm I}}$; (3) the field-flat case,

$$T^{\rm I\to II}_{z_i} = \frac{1}{2}\begin{pmatrix} ({\rm Ai}_{\rm I} - \alpha\,{\rm Ai}'_{\rm I})\exp(-k_{\rm II}z_i) & ({\rm Bi}_{\rm I} - \alpha\,{\rm Bi}'_{\rm I})\exp(-k_{\rm II}z_i) \\ ({\rm Ai}_{\rm I} + \alpha\,{\rm Ai}'_{\rm I})\exp(k_{\rm II}z_i) & ({\rm Bi}_{\rm I} + \alpha\,{\rm Bi}'_{\rm I})\exp(k_{\rm II}z_i)\end{pmatrix} , \qquad \text{(A9)}$$

with $\alpha = [(2m_{\rm I}F_{\rm I})^{1/3}/k_{\rm II}]\frac{m_{\rm II}}{m_{\rm I}}$; and finally, (4) the flat-field case,

$$T^{\rm I\to II}_{z_i} = \pi\begin{pmatrix} ({\rm Bi}'_{\rm II} + \alpha\,{\rm Bi}_{\rm II})\exp(k_{\rm I}z_i) & ({\rm Bi}'_{\rm II} - \alpha\,{\rm Bi}_{\rm II})\exp(-k_{\rm I}z_i) \\ -({\rm Ai}'_{\rm II} + \alpha\,{\rm Ai}_{\rm II})\exp(k_{\rm I}z_i) & -({\rm Ai}'_{\rm II} - \alpha\,{\rm Ai}_{\rm II})\exp(-k_{\rm I}z_i)\end{pmatrix} , \qquad \text{(A10)}$$

with $\alpha = [k_{\rm I}/(2m_{\rm II}F_{\rm II})^{1/3}]\frac{m_{\rm II}}{m_{\rm I}}$.

The transfer matrix across the whole heterostructure, relating the coefficients of the left- to those of the right-hand side, is then simply the product of all interface transfer matrices,

$$T^{l\to r} = T^{r-1\to r}\cdots T^{\rm II\to III}T^{\rm I\to II}T^{l\to \rm I} \ . \qquad \text{(A11)}$$

From a numerical point of view, if rounding and truncation errors become a problem — which is particularly the case for small electric fields — it is more convenient to use another set of transfer matrices which we have illustrated in Fig. 11. Instead of Eq. (A6) we define as transfer matrix

$$T^{z_i\to z_j} = T^{\rm I}_{z_j}\left(T^{\rm I}_{z_i}\right)^{-1} \ , \qquad \text{(A12)}$$

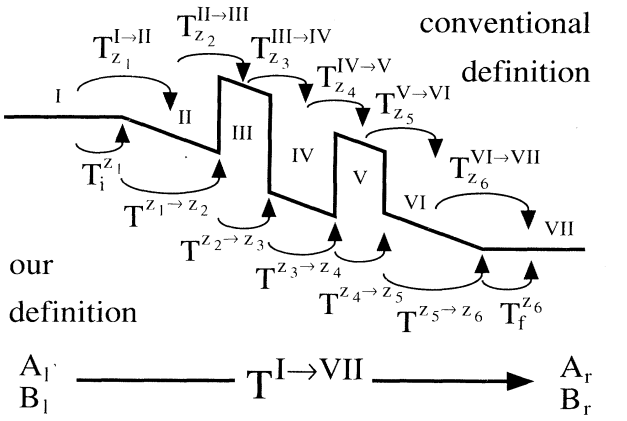

FIG. 11. The "conventional" definition of the transfer matrix is to let it relate the expansion coefficients A and B in the various layers of the structure (upper part). An easier and numerically less complicated way is to define transfer matrices between the values of ψ and ψ' at the interfaces instead (lower part). In order to relate the coefficients A_l, B_l with A_r and B_r, all we need to do is to add two "half" transfer matrices called T_i and T_f, one on each side.

where I is now the layer between the interfaces z_i and z_j. In this way the expansion coefficients of the wave function are not related with each other but rather the values of the wave function and its derivative at the interfaces are related. This approach has a couple of advantages. First of all, the transfer matrices become much simpler, as they now depend on the parameters of one layer instead of two as before, thus leading to only two different types of transfer matrices. In the case of zero electric field, we find

$$T^{z_i\to z_j} = \begin{pmatrix} \cosh(k_{\rm I}\delta z_{ji}) & \frac{m_{\rm I}}{k_{\rm I}}\sinh(k_{\rm I}\delta z_{ji}) \\ \frac{k_{\rm I}}{m_{\rm I}}\sinh(k_{\rm I}\delta z_{ji}) & \cosh(k_{\rm I}\delta z_{ji})\end{pmatrix} , \qquad \text{(A13)}$$

with $\delta z_{ji} = z_j - z_i$. For finite fields the result is

$$T^{z_i\to z_j} = \pi \begin{pmatrix} \mathrm{Ai}(Z_j)\mathrm{Bi}'(Z_i) - \mathrm{Bi}(Z_j)\mathrm{Ai}'(Z_i) & [\mathrm{Ai}(Z_j)\mathrm{Bi}(Z_i) - \mathrm{Bi}(Z_j)\mathrm{Ai}(Z_i)]/\beta_\mathrm{I} \\ \beta_\mathrm{I}\left[\mathrm{Bi}'(Z_j)\mathrm{Ai}'(Z_i) - \mathrm{Ai}'(Z_j)\mathrm{Bi}'(Z_i)\right] & \mathrm{Bi}'(Z_j)\mathrm{Ai}(Z_i) - \mathrm{Ai}'(Z_j)\mathrm{Bi}(Z_i) \end{pmatrix} , \tag{A14}$$

where $\beta_\mathrm{I} = (2m_\mathrm{I}F_\mathrm{I})^{1/3}/m_\mathrm{I}$ and $Z_{i,j} = (2m_\mathrm{I}F_\mathrm{I})^{-2/3}(\hbar^2k_\mathrm{I}^2 - 2m_\mathrm{I}F_\mathrm{I}z_{i,j})$. Eventually, we want to relate the expansion coefficients A_{I_1} and B_{I_1} of the wave function across a series of interfaces $z_i,\ldots,z_j$ to a second set of coefficients, A_{I_2} and B_{I_2}, as we did before in Eqs. (A6) and (A11). To do this we simply have to add an initial matrix in layer I_1 and a final matrix in layer I_2, as illustrated in Fig. 11 for I_1 =I and I_2 =VII,

$$T^{\mathrm{I}_1\to\mathrm{I}_2} = T_f^{z_j}T^{z_m\to z_j}\cdots T^{z_k\to z_l}T^{z_i\to z_k}T_i^{z_i} . \tag{A15}$$

These matrices are defined as

$$T_i^{z_i} = \begin{cases} \begin{pmatrix} \exp(k_\mathrm{I}z_i) & \exp(-k_\mathrm{I}z_i) \\ \frac{k_I}{m_\mathrm{I}}\exp(k_\mathrm{I}z_i) & -\frac{k_\mathrm{I}}{m_\mathrm{I}}\exp(-k_\mathrm{I}z_i) \end{pmatrix}, F_\mathrm{I} = 0 \\ \begin{pmatrix} \mathrm{Ai}(Z_i) & \mathrm{Bi}(Z_i) \\ -\beta_\mathrm{I}\mathrm{Ai}'(Z_i) & -\beta_\mathrm{I}\mathrm{Bi}'(Z_i) \end{pmatrix}, F_\mathrm{I} \neq 0 \end{cases} \tag{A16}$$

where z_i is at the left-hand side of layer I$\equiv \mathrm{I}_1$, and

$$T_f^{z_j} = \begin{cases} \frac{1}{2}\begin{pmatrix} \exp(-k_\mathrm{I}z_j) & \frac{m_\mathrm{I}}{k_\mathrm{I}}\exp(-k_\mathrm{I}z_j) \\ \exp(k_\mathrm{I}z_j) & -\frac{m_\mathrm{I}}{k_\mathrm{I}}\exp(k_\mathrm{I}z_j) \end{pmatrix}, F_I = 0 \\ \pi\begin{pmatrix} \mathrm{Bi}'(Z_j) & -\frac{1}{\beta_\mathrm{I}}\mathrm{Bi}(Z_j) \\ -\mathrm{Ai}'(Z_j) & \frac{1}{\beta_\mathrm{I}}\mathrm{Ai}(Z_j) \end{pmatrix}, F_\mathrm{I} \neq 0 , \end{cases} \tag{A17}$$

with z_j at the right-hand side of layer I$\equiv \mathrm{I}_2$.

2. A low-field expansion

For vanishing electric field, the arguments of the Airy functions in Eq. (A14) diverge, and thus a straightforward comparison with the zero-field case (A13) is not possible. Moreover, this situation is difficult to handle numerically. In this subsection we will outline our method to make contact with the zero-field case. A Taylor expansion of the Airy functions defines four functions $A_1(x,y)$, $A_2(x,y)$, $B_1(x,y)$, and $B_2(x,y)$ by

$$\begin{aligned} \mathrm{Ai}(x+y) &= A_1(x,y)\mathrm{Ai}(x) + A_2(x,y)\mathrm{Ai}'(x) , \\ \mathrm{Bi}(x+y) &= A_1(x,y)\mathrm{Bi}(x) + A_2(x,y)\mathrm{Bi}'(x) , \\ \mathrm{Ai}'(x+y) &= B_1(x,y)\mathrm{Ai}(x) + B_2(x,y)\mathrm{Ai}'(x) , \\ \mathrm{Bi}'(x+y) &= B_1(x,y)\mathrm{Bi}(x) + B_2(x,y)\mathrm{Bi}'(x) . \end{aligned} \tag{A18}$$

The functions A_1, A_2, B_1, and B_2 obey the same differential equations as the Airy functions,

$$\begin{aligned} \frac{d}{dy}A_1(x,y) &= B_1(x,y) \quad , \quad \frac{d}{dy}B_1(x,y) = (x+y)A_1(x,y) , \\ \frac{d}{dy}A_2(x,y) &= B_2(x,y) \quad , \quad \frac{d}{dy}B_2(x,y) = (x+y)A_2(x,y); \end{aligned} \tag{A19}$$

in fact, they are simply linear combinations of Airy functions as can be seen by inverting Eq. (A18). With the help of these functions the transfer matrix of Eq. (A14) can be rewritten as

$$T^{z_i\to z_j} = \begin{pmatrix} A_1(Z_i,\delta Z_{ji}) & -\frac{1}{\beta_\mathrm{I}}A_2(Z_i,\delta Z_{ji}) \\ -\beta_\mathrm{I}B_1(Z_i,\delta Z_{ji}) & B_2(Z_i,\delta Z_{ji}) \end{pmatrix} , \tag{A20}$$

with $\delta Z_{ji} = Z_j - Z_i$. Though the Airy functions diverge for vanishing electric field, the functions A_1, A_2/β_I, $\beta_\mathrm{I}B_1$, and B_2 do not. It is thus very useful to have a low-field expansion for them, instead of using their definitions in terms of the Airy functions. For example, with the aid of a symbolic programming language, it is found that their Taylor expansion consists of subseries of the general form

$$\text{const} \times y^{l+j} \times \sum_n P_{l,j}(n)\frac{(\sqrt{x}y)^{2n}}{(2n+j)!} , \tag{A21}$$

where l and j are some integers and $P_{l,j}(n)$ is a polynom in n. These serieses can be summed up giving functions of $\cosh(\sqrt{x}y)$, $\sinh(\sqrt{x}y)$, and their derivatives. An expansion of the coefficients $A_1(x,y)$, $A_2(x,y)$, $B_1(x,y)$, and $B_2(x,y)$ with respect to the electric field is then obtained by utilizing the asymptotic relations $x = Z_i \propto F^{-2/3}$, $y = \delta Z_{ji} \propto F^{1/3}$, and $\sqrt{x}y \to k\delta z = \text{const}$ for $F \to 0$. When classifying the expansion terms according to these rules we get for up to the fourth order in the electric field F

$$\begin{aligned} A_1(x,y) = {} & \Big(1 - \frac{y}{4x} + \frac{7y^2}{32x^2} + \frac{y^4}{32x} - \frac{35y}{128x^4} - \frac{35y^3}{192x^3} - \frac{7y^5}{384x^2} + \frac{1365y^2}{2048x^5} + \frac{1085y^4}{6144x^4} + \frac{119y^6}{9216x^3} + \frac{y^8}{6144x^2}\Big)\cosh(\sqrt{x}y) \\ & + \Big(\frac{1}{4x} + \frac{y^2}{4} - \frac{7y}{32x^2} - \frac{5y^3}{48x} + \frac{35}{128x^4} + \frac{35y^2}{128x^3} + \frac{7y^4}{96x^2} + \frac{y^6}{384x} \\ & - \frac{1365y}{2048x^5} - \frac{1225y^3}{3072x^4} - \frac{175y^5}{3072x^3} - \frac{y^7}{512x^2}\Big)\frac{1}{\sqrt{x}}\sinh(\sqrt{x}y) , \end{aligned}$$

$$\begin{aligned} A_2(x,y) = {} & \Big(\frac{y^2}{4x} - \frac{5y}{32x^3} - \frac{5y^3}{48x^2} + \frac{35y^2}{128x^4} + \frac{25y^4}{384x^3} + \frac{y^6}{384x^2} - \frac{1155y}{2048x^6} - \frac{385y^3}{1024x^5} - \frac{161y^5}{3072x^4} - \frac{y^7}{512x^3}\Big)\cosh(\sqrt{x}y) \\ & + \Big(1 - \frac{y}{4x} + \frac{5}{32x^3} + \frac{5y^2}{32x^2} + \frac{y^4}{32x} - \frac{35y}{128x^4} - \frac{5y^3}{32x^3} - \frac{7y^5}{384x^2} \\ & + \frac{1155}{2048x^6} + \frac{1155y^2}{2048x^5} + \frac{1015y^4}{6144x^4} + \frac{113y^6}{9216x^3} + \frac{y^8}{6144x^2}\Big)\frac{1}{\sqrt{x}}\sinh(\sqrt{x}y) , \end{aligned}$$

$$B_1(x,y) = \left(\frac{y^2}{4} + \frac{7y}{32x^2} + \frac{y^3}{48x} - \frac{35y^2}{128x^3} - \frac{7y^4}{384x^2} + \frac{y^6}{384x} + \frac{1365y}{2048x^5} + \frac{315y^3}{1024x^4} + \frac{21y^5}{1024x^3} - \frac{y^7}{1536x^2}\right)\cosh(\sqrt{x}y)$$
$$+\left(1 + \frac{y}{4x} - \frac{7}{32x^3} - \frac{3y^2}{32x^2} + \frac{y^4}{32x} + \frac{35y}{128x^4} + \frac{7y^3}{64x^3} - \frac{y^5}{384x^2}\right.$$
$$\left. - \frac{1365}{2048x^6} - \frac{1085y^2}{2048x^5} - \frac{665y^4}{6144x^4} - \frac{7y^6}{9216x^3} + \frac{y^8}{6144x^2}\right)\sqrt{x}\sinh(\sqrt{x}y) \ ,$$

$$B_2(x,y) = \left(1 + \frac{y}{4x} - \frac{5y^2}{32x^2} + \frac{y^4}{32x} + \frac{35y}{128x^4} + \frac{5y^3}{48x^3} - \frac{y^5}{384x^2} - \frac{1155y^2}{2048x^5} - \frac{595y^4}{6144x^4} - \frac{13y^6}{9216x^3} + \frac{y^8}{6144x^2}\right)\cosh(\sqrt{x}y)$$
$$+\left(\frac{-1}{4x} + \frac{y^2}{4} + \frac{5y}{32x^2} + \frac{y^3}{48x} - \frac{35}{128x^4} - \frac{25y^2}{128x^3} - \frac{5y^4}{192x^2} + \frac{y^6}{384x}\right.$$
$$\left. + \frac{1155y}{2048x^5} + \frac{875y^3}{3072x^4} + \frac{65y^5}{3072x^3} - \frac{y^7}{1536x^2}\right)\frac{1}{\sqrt{x}}\sinh(\sqrt{x}y) \ .$$

It can easily be verified that this expansion satisfies Eq. (A18) up to the fourth order in the electric field, and that for vanishing field Eq. (A20) reduces to the zero-field result (A13). Its usefulness depends on the parameters of the RTD/MQW structure, but from our experience it seems to cover a range of a few hundred V/cm for reasonable choices of parameters.

3. A brief description of the numerical method

Having provided an iterative definition of the analytic result for the derivative of the inverse transmission amplitude, $t^{-1}(E)$, the roots of $t^{-1}(E)$ were found by using a standard Newton root finder in the complex-energy plane. When changing the electric field, "tracks" of roots were generated by extrapolating the new root first and then using this value as a starting point for the root finder. In this way it was possible to keep track of the various quantum levels in a heterostructure, even when their quasieigenenergies came to resonance. To avoid running over an (anti)crossing of two quantum levels by using a too large step size in the electric field, the likely positions of these (anti)crossing events (as well as possible crossings with the conduction-band edges) were estimated before each step, and the next step size correspondingly chosen.

*Present address: Hitachi Cambridge Laboratory, Madingley Road, Cambridge CB3 OHE, UK.

[1]B. Deveaud, J. Shah, T.C. Damen, B. Lambert, and A. Regreny, Phys. Rev. Lett. **58**, 2582 (1987).
[2]M. Tsuchiya, T. Matsusue, and H. Sakaki, Phys. Rev. Lett. **59**, 2356 (1987).
[3]J. Shah, in *Hot Carriers in Semiconductor Nanostructures: Physics and Applications*, edited by J. Shah (Academic Press, Boston, 1992), p. 279.
[4]G. Livescu, A.M. Fox, D.A.B. Miller, T. Sizer, W.H. Knox, A.C. Gossard, and J.H. English, Phys. Rev. Lett. **63**, 438 (1989).
[5]A.M. Fox, D.A.B. Miller, G. Livescu, J.E. Cunningham, and W.Y. Jan, IEEE J. Quantum Electron. **27**, 2281 (1991).
[6]Nanzhi Zou, J. Rammer, and K.A. Chao, Phys. Rev. B **46**, 15912 (1992).
[7]Care should be taken not to confuse the *lifetime* of a resonance with the various tunneling times, such as "phase time," "dwell time," "Landauer-Büttiker time," or "Larmor time," corresponding to different experimental setups, as is excellently discussed by A.P. Jauho, in *Hot Carriers in Semiconductor Nanostructures: Physics and Applications*, edited by J. Shah (Academic Press, Boston, 1992), p. 121.
[8]S. Luryi, Appl. Phys. Lett. **47**, 490 (1985).
[9]T. Tada, A. Yamaguchi, T. Ninomiya, H. Uchiki, T. Kobayashi, and T. Yao, J. Appl. Phys. **63**, 5491 (1988).
[10]T.B. Norris, X.J. Song, W.J. Schaff, L.F. Eastman, G. Wicks, and G.A. Mourou, Appl. Phys. Lett. **54**, 60 (1989).
[11]D.Y. Oberli, J. Shah, T.C. Damen, C.W. Tu, T.Y. Chang, D.A.B. Miller, J.E. Henry, R.F. Kopf, N. Sauer, and A.E. DiGiovanni, Phys. Rev. B **40**, 3028 (1989).
[12]M. Nido, M.G.W. Alexander, W.W. Rühle, T. Schweizer, and K. Köhler, Appl. Phys. Lett. **56**, 355 (1990).
[13]N. Shimizu, T. Furuta, T. Waho, and T. Mizutani, Jpn. J. Appl. Phys. Part 2 **29**, L1757 (1990).
[14]N. Harada and S. Kuroda, Jpn. J. Appl. Phys. Part 2 **25**, L871 (1986).
[15]P.J. Price, Superlatt. Microstruct. **2**, 593 (1986).
[16]E.J. Austin and M. Jaros, Appl. Phys. Lett. **47**, 274 (1985).
[17]M.K. Jackson, M.B. Johnson, D.H. Chow, T.C. McGill, and C.W. Nieh, Appl. Phys. Lett. **54**, 552 (1989).
[18]Th.B. Bahder, C.A. Morrison, and J.D. Bruno, Appl. Phys. Lett. **51**, 1089 (1987).
[19]P.J. Price, Phys. Rev. B **38**, 1994 (1988).
[20]P.F. Bagwell and R.K. Lake, Phys. Rev. B **46**, 15329 (1992).
[21]P.J. Price, IEEE Trans. Electron Devices **39**, 520 (1992).
[22]Y. Zohta and H. Ezawa, J. Appl. Phys. **72**, 3584 (1992).
[23]One might expect that since the Hamiltonian is Hermitian, no complex eigenvalues are possible. However, we can equally well think of the imaginary part of the eigenenergy as being part of the potential V ("optical potential"). The non-normalizability of the wave functions means that in matrix elements such as $\langle 1|O|2\rangle$ in general it makes a difference whether the operator O is applied to the left- or the right-hand side (a partial integration now involves a nonvanishing surface integral at infinity).
[24]Similar results for truly bound levels were reported in B. Olejníková, Semicond. Sci. Technol. **8**, 525 (1993).

[25]Strictly speaking, for all quantum levels except for truly bound levels the squared wave-function amplitude $|\psi(z)|^2$ cannot be interpreted as a probability function, as in all these cases the wave function $\psi(z)$ cannot be normalized to unity. However, for the purpose of the present discussion only *relative* amplitudes are relevant, and we have therefore used the simplest possible normalization in a box covering the whole structure from one contact to the other. The resulting amplitudes depend only very weakly on the precise size of this box, as the amplitudes at the contacts are typically many orders of magnitude smaller than those in the quantum wells.

[26]R. Tsu and L. Esaki, Appl. Phys. Lett. **22**, 562 (1973).

[27]See, for instance, C. Cohen-Tannoudji, B. Diu, and F. Laloë, *Quantum Mechanics* (Wiley-Interscience, New York, 1977), Vol. 1, p. 477.

[28]The definition of these matrix elements is somewhat subtle for complex-energy wave functions as noted in Ref. 23, but for the purpose of a qualitative discussion it is sufficient to use a cutoff at the contacts or a convolution of the wave functions in the contacts with a strongly decaying function. Other definitions of the basis set $\{|\phi_1\rangle, |\phi_2\rangle\}$ can, for instance, be based on some variation of the tunneling-Hamiltonian approach [J. Bardeen, Phys. Rev. Lett. **6**, 57 (1961); E.O. Kane, in *Tunneling Phenomena in Solids*, edited by E. Burstein and S. Lundquist (Plenum, New York, 1969), p. 1].

[29]This result is of interest when utilizing a line-shape analysis of the transmission probability $T(E)$ to extract the intrinsic lifetime of a resonance. As mentioned earlier, such an approach is only possible when the quasieigenenergy is above the conduction-band edge in *both* contacts, which rules out many applications in MQW structures where the energy levels are below the emitter band edge. However, in the light of the results discussed above, we can modify such a MQW structure in a way that the emitter contact is replaced by a contact similar to that shown in Fig. 10. The barrier height $E_{c'}$ is taken to be equal to the emitter conduction-band edge of the original MQW, while E_c is set to its collector band edge. Effectively, this modified structure is at zero external bias, and in particular, the transmission probability $T(E)$ will be *finite*. Hence a standard line-shape analysis can be applied, which in the limit of $L \to \infty$ will approach the complex-energy result for the correct boundary conditions, as is expected on physical grounds.

[30]M. Wagner and H. Mizuta, Jpn. J. Appl. Phys. Part 2 **32**, L520 (1993); M. Wagner and H. Mizuta, Appl. Phys. Lett. (to be published).